Optimization of the Microcrystalline Silicon Deposition Efficiency

B. Strahm*, A. A. Howling, L. Sansonnens, and Ch. Hollenstein

Ecole Polytechnique Fédérale de Lausanne (EPFL),

Centre de Recherches en Physique des Plasmas, CH-1015 Lausanne, Switzerland.

(Dated: September 21, 2006)

Abstract

Cost reduction constraints for microcrystalline silicon thin film photovoltaic solar cells require high deposition rates and high silane gas utilization efficiencies. If the requirements in deposition rate have sometimes been fulfilled, it is generally not the case for the silane utilization. In this work, a reactor-independent methodology has been developed to determine the optimum plasma parameters in terms of deposition rate, silane utilization and material microstructure. Using this optimization method in an industrial large area plasma-enhanced chemical vapor deposition reactor, a microcrystalline layer has been deposited at a rate of 10.9 Å/s, with a silane utilization efficiency above 80 %. Results have shown that the highest deposition efficiency is obtained with high silane input concentration and not with the common highly hydrogen-diluted deposition regime.

* Electronic mail: benjamin.strahm@epfl.ch

I. INTRODUCTION

Since the first deposition of microcrystalline hydrogenated silicon (μc-Si:H) by radio frequency (RF) glow discharge in 1979 by Ushui *et al*[1], intensive investigations have been performed to determine the optimum plasma parameters to produce it. The particular interest in μc-Si:H compared to amorphous hydrogenated silicon (a-Si:H) is due to its superior stability under light exposure[2], which is important for photovoltaic applications; however, it is difficult to deposit at high rate. The conventional way to produce μc-Si:H layers by plasma-enhanced chemical vapor deposition (PECVD) is to strongly dilute the silane (SiH_4) with hydrogen, to reach a few percent silane concentration in contrast to the low-dilution regime in which a-Si:H is commonly deposited[3,4]. This accepted technique is used in order to supply the high quantity of atomic hydrogen in the plasma required to produce μc-Si:H[5]. Within this highly-diluted regime, there are many experimental investigations into the role of the different plasma parameters such as the RF power[6], excitation frequency[7], pressure[8], silane concentration[9] and gas flow rates[10]. However, although very high deposition rates have sometimes been reported[11], these studies are strongly reactor dependent and no multi-parametric experimental methodology has been developed. Moreover, for suitable industrial photovoltaic solar cell manufacture, the production costs have to be minimized, meaning that not only the deposition rate of μc-Si:H has to be maximized, but also that the utilization fraction of the silane gas (≈ 500 \$/kg) has to be as high as possible. Up to now, processes for the deposition of amorphous and microcrystalline silicon from the low silane concentration regime show poor silane utilization even if deposition rates are high[12].

Previous experiments and simple plasma chemistry modeling[13] have shown that high deposition efficiency, i.e. high gas utilization efficiency, can only be reached when high silane input concentration (> 30 %) is used. Moreover, these results have shown that this was not incompatible with low silane concentration *in the plasma*[14,15] because the silane is highly depleted for discharge conditions suitable for microcrystalline silicon deposition. Hence, microcrystalline films can be grown even using pure silane discharges[13,16] if the plasma parameters are correctly selected. However, it is probably not advisable to work with the extreme case of pure silane gas to obtain a material of good quality deposited at high rate, because of limitations due to polysilanes and powder formation consuming silane in channels other than film growth[13].

The aim of this work is to establish a reactor-independent methodology to determine the optimum plasma conditions in terms of deposition rate, silane utilization fraction and material microstructure. The industrial type reactor described in section II was used to demonstrate the optimization method introduced in sections III A and III B. Fourier transform infrared spectroscopy was used to measure the silane concentration in the plasma during the different phases of the optimization. Finally, a flow diagram including the selection of the initial parameters and an optimization procedure requiring only deposition rate and crystallinity measurements is proposed in section III C.

II. THE EXPERIMENTAL ARRANGEMENT

The deposition reactor used in this work is a modified version of the industrial KAI-S reactor from Unaxis Ltd based on the PlasmaBox® concept[13,15,17]. It consists of a 47 x 57 cm² grounded aluminum box inside which the RF electrode is suspended at a distance of 18 mm from the grounded base. The RF electrode acts also as a gas showerhead distributing the gas uniformly[18] over the whole 3 mm thick glass substrate area (37 x 47 cm²). The temperature of the electrodes was fixed at 230 °C. The other deposition parameters are discussed in section (III A). The system was also equipped with Fourier transform infrared absorption spectroscopy installed in the exhaust line with a pass length of 1 m between two ZnSe windows[13,15,19] which was used to measure the partial pressure of silane in the pumping line using a calibration curve performed with pure silane gas without plasma[15]. Hence, the silane concentration in the plasma, c_p, can be measured and is defined as:

$$c_\mathrm{p} = p_{\mathrm{SiH_4}}/p, \tag{1}$$

and the silane input concentration, c, as:

$$c = p_{\mathrm{SiH_4}}^0/p, \tag{2}$$

where $p_{\mathrm{SiH_4}}$ and $p_{\mathrm{SiH_4}}^0$ are the silane partial pressure with and without plasma in the reactor, respectively, and p is the total pressure, which is controlled by a butterfly valve. The relation between these two concentrations for a uniform gas showerhead[18] and a uniform plasma is:

$$c_p = (1 - D)c, \tag{3}$$

where $D = (p^0_{\text{SiH}_4} - p_{\text{SiH}_4})/p^0_{\text{SiH}_4}$ is the silane depletion fraction in the plasma. The deposition rate was measured *in situ* from the back of the substrate by monochromatic light interferometry through a hole at the center of the grounded electrode. The film crystallinity was measured by micro-Raman spectroscopy as described elsewhere[15].

III. RESULTS

A. Process parameter selection

This section shows how to select the process parameters (RF power, excitation frequency, gas flow rates and pressure) which will give the appropriate starting point of the process optimization technique presented in section III B.

1. RF power

Generally, the RF power input for μc-Si:H deposition is set to the maximum possible value for two main reasons: (i) the deposition rate increases with the RF power density[20] (in the absence of polysilane and powder formation) due to the increase of the silane depletion D[13,15]; (ii) for the same reason, the silane concentration in the plasma, c_{p}, is lower meaning that the silane in the plasma is more strongly-diluted with hydrogen, hence, the deposited material is more crystalline[13,15]. However, we have to take into account a potential up-scaling from this laboratory reactor to a larger area industrial reactor for mass production of solar cells. For example, a process developed in a small reactor with an excessively-high RF power density will not be suitable for solar cell production. The RF power input used here was 1000 W (0.37 W·cm^{-2}), which is not the highest deliverable power of our generator, nor the maximum power rating of our system (including matching box and reactor), but corresponds to a power density which can be easily implemented in existing larger industrial reactors.

2. Excitation frequency

According to previous studies, the excitation frequency should be set as high as possible, because of the higher deposition rates[7,21] and higher silane depletion fractions[19] leading to

films containing a larger crystalline fraction at very high frequencies[15] (VHF). Moreover, the reduction of the ion bombardment energy of the film surface reduces the internal stress of the film and improves the material quality[5]. However, as for the input RF power, upscaling to industrial reactors limits the increase of the excitation frequency due to standing wave non-uniformities[22–25] as observed in large area reactors unless special precautions are taken[24]. For all these reasons an excitation frequency of 40.68 MHz has been chosen in this work.

3. Gas flow rates

The silane flow rate is a key parameter and has to be carefully chosen for two reasons: (i) a flow too small will limit the deposition rate due to the insufficient available raw material; (ii) on the other hand, a flow too high will lead to a low silane utilization efficiency and a large fraction of wasted raw material, increasing the cost of the final product. Hence, the choice of the silane flow rate will depend on the target deposition rate, R_{target}, the target silane utilization efficiency, u_{target}, and on the reactor size given by the total deposition area, A. Undissociated silane, polysilanes and powder formed in the plasma are pumped out without contributing to the film growth, making the silane utilization efficiency u less than perfect, $u < 1$. Assuming that the film is uniformly deposited, the silane flow rate can be determined as follows[13,15]:

$$F_{\text{SiH}_4}[\text{sccm}] = 10.4 \cdot \frac{R_{\text{target}}[\text{Å/s}]}{u_{\text{target}}} \cdot A \text{ [m}^2]. \tag{4}$$

R_{target} and u_{target} cannot be arbitrarily selected. If the chosen values are too high, it may be impossible to attain them, necessitating a new optimization with lower values of R_{target} and/or u_{target} as will be shown in section III C. For the KAI-S reactor presented in section II, for a target deposition rate of 10 Å/s, the silane flow rate is 80 sccm if we suppose a silane utilization efficiency $u_{\text{target}} = 0.75$. If there were no silane wastage ($u = 1$), the maximum possible deposition rate R_{max} would be 13.3 Å/s for this example. The measured silane utilization efficiency is the ratio of the measured deposition rate to the maximum possible deposition rate (R/R_{max}).

In order to start the optimization of the process in a powder free regime, the hydrogen flow has to be sufficiently high (i.e. the silane concentration sufficiently low) to begin in the

standard highly hydrogen-diluted regime for transition material with silane concentration typically less than 3 %[15]. It was fixed here at 2700 sccm, corresponding to an initial silane concentration of 2.9 %.

4. Pressure

The deposition rate depends on the working pressure, especially around 1 - 2 mbar, where a strong increase with pressure has been observed in different reactors[13,26,27]. High pressure is also important in terms of crystallinity[10] due to the increase of the silane depletion fraction with pressure[15] due to a longer residence time. An additional advantage of high pressure is that the ion bombardment energy is reduced in a collisional sheath, and hence the film quality improved. However, to avoid powder formation, the working pressure should not be too high[28]. The starting point pressure was fixed at 2 mbar in order to benefit from the high deposition rate and to avoid powder formation. Note that the choice of the initial pressure depends on the inter-electrode distance, for example, in narrow gap reactors ($\approx$ 10 mm) plasma ignition is difficult for pressures below about 4 mbar. For the current reactor with a 18 mm gap, the initial pressure should be 2 mbar or more.

B. Optimization of the silane gas utilization

The process optimization presented in this section has been developed in order to be used even if the deposition reactor is not equipped with an IR absorption measurement. It requires only a deposition rate measurement (*in situ* or *ex situ*) and a film crystallinity measurement (Raman spectroscopy, XRD, ...). Figure 1 presents the microstructure dependence on the silane depletion and silane input concentration. The flux ratio of atomic hydrogen to silicon radicals to the surface and therefore the material crystallinity are expected to remain constant if the silane concentration in the plasma, c_p, remains constant, as demonstrated by Strahm *et al*[15]. A zone of constant crystallinity, chosen to correspond to the deposition of transitional material in Fig. 1, is therefore delimited by contours of constant silane concentration in the plasma, $c_p = (1 - D)c = $ constant. For higher values of c_p the deposited material is amorphous, and for lower values of c_p it is microcrystalline. The material in the transition zone itself can be either amorphous or microcrystalline, because

6

at the microstructure transition, c_{p} is not the only parameter determining the crystallinity. Since the material of interest for solar cell applications is μc-Si:H grown at the boundary between a-Si:H and μc-Si:H[29], the process conditions of interest are in the microstructure transition zone presented in Fig. 1.

As described in the previous section, the starting parameters of the optimization are a RF power input of 1000 W, an excitation frequency of 40.68 MHz, a silane flow rate of 80 sccm, a hydrogen flow rate of 2700 sccm and a pressure of 2 mbar. With such parameters, the starting process had a silane depletion fraction D of 0.31 as shown in Fig. 1, and the resulting film had a Raman crystallinity of 55 %. The deposition rate was 2.8 Å/s, corresponding to a silane utilization efficiency R/R_{max} of 21.4 %. Since the RF power input, the excitation frequency and the silane flow rate are fixed according to sec. III A, the two remaining adjustable parameters are the pressure, p, and the hydrogen flow rate, $F_{\mathrm{H_2}}$. These two parameters can be varied separately, giving contours of iso-p (variable $F_{\mathrm{H_2}}$) or iso-$F_{\mathrm{H_2}}$ (variable p).

Figure 2 shows that reducing the hydrogen flow rate $F_{\mathrm{H_2}}$, while keeping the silane flow rate and the pressure constant, increases the deposition rate and, hence, the silane utilization efficiency R/R_{max} from 21.4 % to 31.1 % for hydrogen flow rates of 2700 and 1000 sccm, respectively. This increase of the silane utilization efficiency with silane input concentration is mainly because the total flow rate reduction, due to the decrease of $F_{\mathrm{H_2}}$ at constant $F_{\mathrm{SiH_4}}$, increases the gas residence time and hence the silane depletion in the plasma. The variation of c and D with the hydrogen flow rate (Fig. 2(a)) can be deduced from the chemistry model presented in previous work[15], for constant plasma dissociation frequency, pressure and silane flow rate. The curve presented in Fig. 2(a) is given by

$$c = \frac{-1 + \sqrt{1 + 4\mathrm{B}D}}{2(1 - D)}, \tag{5}$$

where B is a constant depending on the dissociation frequency, pressure and silane flow rate. The silane concentration, c, is varied by decreasing the hydrogen flow rate, $F_{\mathrm{H_2}}$. However, reducing the hydrogen flow rate does not guarantee a constant crystallinity of the deposited material. Indeed, by following the iso-p curves from low to high silane concentration, the contour moves away from the microstructure transition zone[13,15], making the deposited material more amorphous as shown in Fig. 2.

The working pressure p, which is the only other adjustable parameter, can be used to

move back to the microstructure transition zone by changing the pumping speed while leaving the gas flow rates constant (Fig. 3(a)). This pressure variation changes the silane depletion fraction without changing the silane concentration as shown by the horizontal line in Fig. 3(a). This increase of the silane depletion fraction with the working pressure is mainly due to the increase of the gas residence time caused by the pumping speed reduction. Moreover, as shown in Fig. 3(b) the increase of the silane depletion with the pressure has two beneficial effects: (i) it increases the deposition efficiency and hence the deposition rate and (ii) the silane concentration in the plasma, c_{p}, is reduced, making the deposited material more crystalline.

Hence, by increasing step-by-step the dissociation efficiency by alternatively reducing the hydrogen flow rate $F_{\mathrm{H_2}}$ (at constant p) and by increasing the pressure p (at constant $F_{\mathrm{H_2}}$) as shown by the data points in Fig. 4, it is possible to remain in the microstructure transition zone while increasing the deposition rate.

C. Flow diagram

Following the conclusions of the previous sections, a process flow diagram can be drawn up for the optimization of the deposition efficiency of microcrystalline silicon. The only necessary equipment required to follow the flow diagram presented here are an *in situ* or *ex situ* deposition rate measurement and a film crystallinity measurement such as Raman spectroscopy or X-Ray diffraction (XRD). The method can be separated into two blocks which are the selection of the initial parameters and the process optimization as sketched in Fig.5.

The first step is to define the initial plasma parameters (RF power, excitation frequency and pressure) as described in section III A. The silane flow rate can be calculated through Eq. 4 after having defined a target deposition rate, R_{target}, and a target silane utilization fraction, u_{target}. In order to start the optimization in a powder free regime, the silane concentration has to be low ($< 3 \%$), hence a large hydrogen flow will be chosen.

The optimization phase begins with the deposition of a film with the initial plasma parameters. Two cases can occur: the film can be microcrystalline or amorphous. In the first case, the deposition rate has to be increased by reducing the hydrogen flow rate (keeping all the other plasma parameters constant). This reduction of $F_{\mathrm{H_2}}$ is continued until

8

the deposited layer becomes amorphous, corresponding to the second case. To go back to the transition material from the amorphous region, the pressure has to be increased in order to reduce the silane concentration in the plasma by increasing the silane depletion as shown in the previous section. If the deposition rate increases, this step has to be repeated until the film again becomes microcrystalline, corresponding to the first case. The optimization is performed by alternating phases in which the hydrogen flow is reduced and phases in which the pressure is increased until the deposition rate no longer increases. In such a case, if the deposition rate is higher than the target deposition rate R_{target} all objectives are fulfilled and the last microcrystalline process conditions are maintained, or the optimization can be continued by using a higher target deposition rate. Otherwise, if the deposition rate R is lower than R_{target}, it means that the experimental silane utilization fraction u was smaller than the target utilization fraction u_{target} in Eq. 4. This can be due to undissociated silane, or to dissociated silane transformed into polysilanes and powder, which are pumped out of the system[13]. This means that R_{target} and/or u_{target} have been overestimated and cannot be attained for the deposition system used. Then R_{target} and/or u_{target} in Eq. 4 must be reduced, the silane flow rate updated, and the optimization restarted. Note that the deposition rate may be faster in reducing u_{target}, but that the silane utilization efficiency may be higher in reducing R_{target}.

Following the optimization flow diagram presented in Fig. 5, a microcrystalline silicon film with a Raman crystallinity of 66 % was deposited at a deposition rate of 10.9 Å/s as shown in Fig. 3(a), which is higher than the initial target deposition rate (10 Å/s), and corresponds to a silane utilization efficiency of 82.3 %, which is higher than the target utilization fraction (75 %).

IV.   CONCLUSIONS

An optimization procedure has been developed to determine the optimum plasma conditions in terms of deposition rate, silane utilization fraction and material crystallinity. Results have shown that if the initial plasma parameters are carefully selected, the deposition process can be optimized by varying only the working pressure and the hydrogen flow rate. It has been shown that for the deposition of μc-Si:H, the highest silane utilization efficiency is obtained towards pure silane and not towards the common highly hydrogen-diluted regime.

The optimization methodology has been used to reach a deposition rate of 10.9 Å/s of a material with a crystalline fraction of 66 % and a silane utilization efficiency of 82.3 %.

Acknowledgments

---

[1] M. Usui, S. Kikuchi, J. Non-Cryst. Solids **34**, 1 (1979).

[2] J. Meier, R. Flückiger, H. Keppner, and A. Shah, Appl. Phys. Lett. **65**, 860 (1994).

[3] U. Kroll, C. Bucher, S. Benagli, I. Schönbächler, J. Meier, A. Shah, J. Ballutaud, A. A. Howling, C. Hollenstein, A. Büchel, et al., Thin Solid Films **451-452**, 525 (2004).

[4] T. Nishimoto, M. Takai, H. Miyahara, M. Kondo, and A. Matsuda, J. Non-Cryst. Solids **299-302**, 1116 (2002).

[5] A. Matsuda, J. Non-Cryst. Solids **338-340**, 1 (2004).

[6] H. Yang, C. Wu, J. Huang, R. Ding, Y. Zhao, X. Geng, and S. Xiong, Thin Solid Films **472**, 125 (2005).

[7] E. Amanatides, D. Mataras, and D. E. Rapakoulias, Thin Solid Films **383**, 15 (2001).

[8] D. Mataras, Pure Appl. Chem. **77**, 379 (2005).

[9] S. Klein, T. Repmann, and T. Brammer, Solar Energy **77**, 893 (2004).

[10] M. Fukawa, S. Suzuki, L. Guo, M. Kondo, and A. Matsuda, Solar Energy Mat. Solar Cells **66**, 217 (2001).

[11] H. Takatsuka, M. Noda, Y. Yonekura, Y. Takeuchi, and Y. Yamauchi, Solar Energy **77**, 951 (2004).

[12] T. Roschek, B. Rech, J. Müller, R. Schmitz, and H. Wagner, Thin Solid Films **451-452**, 466 (2004).

[13] B. Strahm, A. A. Howling, L. Sansonnens, C. Hollenstein, U. Kroll, J. Meier, C. Ellert, L. Feitknecht, and C. Ballif, submitted to Solar Energy Mat. Solar Cells (2006).

[14] A. Howling, L. Sansonnens, J. Ballutaud, F. Grangeon, T. Delachaux, C. Hollenstein, V. Daudrix, and U. Kroll, in *16th European Photovoltaic Solar Energy Conference* (Glasgow (UK),

2000), p. 375.

[15] B. Strahm, A. A. Howling, L. Sansonnens, and C. Hollenstein, submitted to Plasma Source Sci. Technol. (2006).

[16] M. N. Van den Donker, B. Rech, F. Finger, W. M. M. Kessels, and M. C. M. van den Sanden, Appl. Phys. Lett. **87**, 263503 (2005).

[17] J. Perrin, J. Schmitt, C. Hollenstein, A. A. Howling, and L. Sansonnens, Plasma Phys. and Controlled Fusion **42**, B353 (2000).

[18] L. Sansonnens, A. A. Howling, and C. Hollenstein, Plasma Sources Sci. Technol. **9**, 205 (2000).

[19] L. Sansonnens, A. A. Howling, and C. Hollenstein, Plasma Sources Sci. Technol. **7**, 114 (1998).

[20] R. C. Ross and J. Jaklik Jr, J. Appl. Phys. **55**, 3785 (1983).

[21] A. A. Howling, J.-L. Dorier, C. Hollenstein, U. Kroll, and F. Finger, J. Vac. Sci. Technol. **A 10**, 1080 (1992).

[22] M. A. Lieberman, J. P. Booth, P. Chabert, J. M. Rax, and M. M. Turner, Plasma Sources Sci. Technol. **11**, 283 (2002).

[23] L. Sansonnens, A. A. Howling, and C. Hollenstein, Plasma Sources Sci. Technol. **15**, 302 (2006).

[24] H. Schmidt, L. Sansonnens, A. A. Howling, and C. Hollenstein, J. Appl. Phys. **95**, 4559 (2004).

[25] L. Sansonnens, A. Pletzer, D. Magni, A. A. Howling, C. Hollenstein, and J. P. M. Schmitt, Plasma Sources Sci. Technol. **6**, 170 (1997).

[26] U. Graf, J. Meier, U. Kroll, J. Bailat, E. Vallat-Sauvain, and A. Shah, Thin Solid Films **427**, 37 (2003).

[27] B. Rech, T. Roschek, J. Müller, S. Wieder, and H. Wagner, Solar Energy Mat. Solar Cells **66**, 267 (2001).

[28] M. van den Donker, E. Hamers, and G. Kroesen, J. Phys. D: Appl. Phys. **38**, 2382 (2005).

[29] G. M. Ferreira, A. S. Ferlauto, C. Chen, R. J. Koval, J. M. Pearce, C. Ross, C. R. Wronski, and R. W. Collins, J. Non-Cryst. Solids **338-340**, 13 (2004).

Figure Captions

FIG. 1: Microstructure dependence on silane depletion fraction and silane input concentration. The shaded microstructure transition zone is delimited by two contours of constant silane concentration in the plasma, $c_{\mathrm{p}} = \mathrm{constant}$[15]. To avoid powder formation, the starting point of the optimization is in the highly H_2-diluted regime.

FIG. 2: (a) Variation of D and c when the hydrogen flow is decreased, while the silane flow rate and the pressure are kept constant (B = 0.052). (b) Deposition rate ($\circ$) and Raman crystallinity ($\bullet$) as a function of the measured silane concentration with a constant silane flow rate of 80 sccm and a constant pressure of 2 mbar. The lines are used as guidelines.

FIG. 3: (a) Effect of a pressure increase on c and D. (b) Deposition rate ($\circ$) and Raman crystallinity ($\bullet$) as a function of the working pressure with constant silane and hydrogen flow rates of 80 and 150 sccm, respectively. The lines are used as guidelines.

FIG. 4: Multi-step experimental results following iso-p and iso-F_{H_2} (B = 0.002 − 6) curves from low to high silane concentration and depletion fraction.

FIG. 5: Flow diagram for μc-Si:H deposition optimization, with first the selection of initial plasma parameters and second the procedure to optimize the deposition efficiency of transitional material.
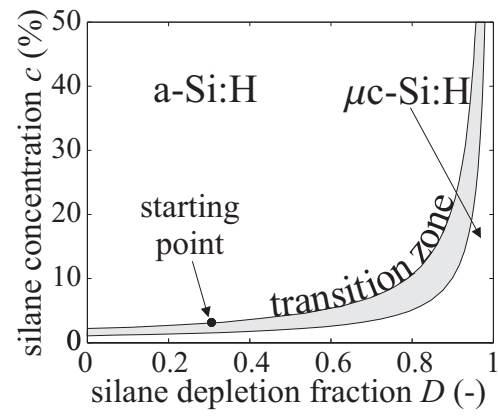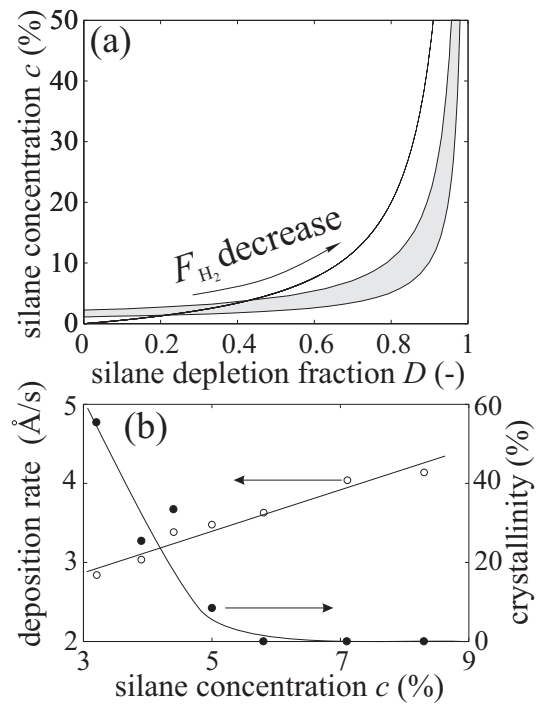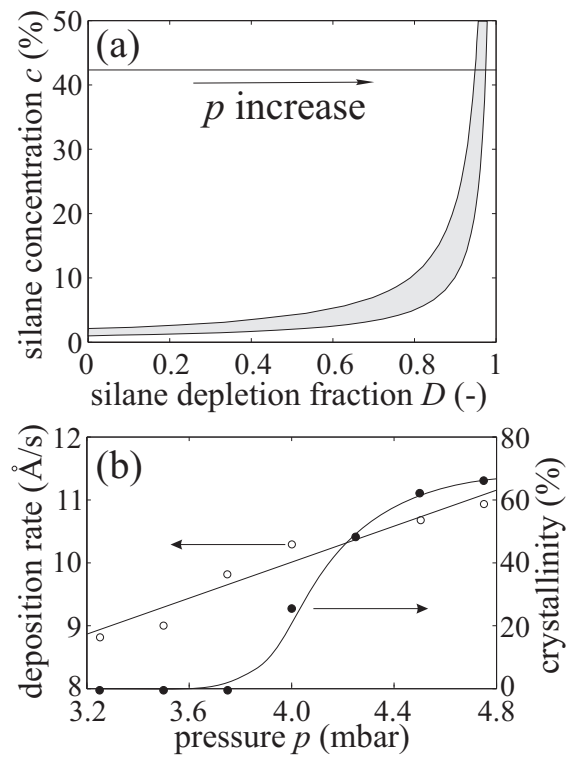
Figure 1 of paper TF-WeM6

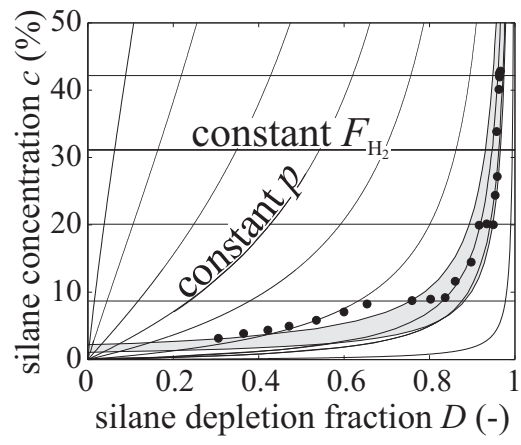Figure 2 of paper TF-WeM6

Figure 3 of paper TF-WeM6

Figure 4 of paper TF-WeM6

Determine
technical limits
(power and
frequency)

Select initial parameters:
$c < 3\ \%$
$R_{target},\ l,\ F_{SiH_4},\ F_{H_2},\ p$

Crystalline ?

Yes

No

decrease F_{H_2}

increase p

Does R increase ?

No

Yes

$R \geqslant R_{target}$

$R < R_{target}$
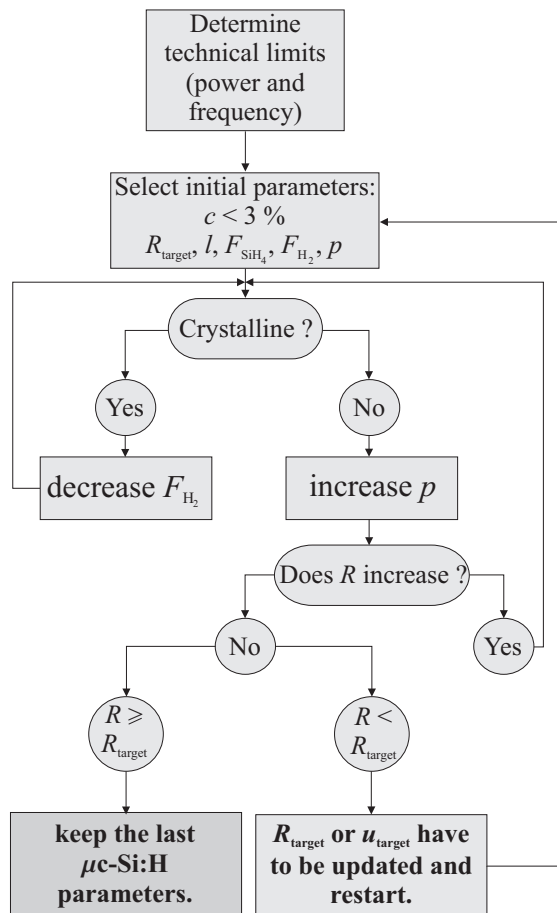
keep the last
μc-Si:H
parameters.

R_{target} or u_{target} have
to be updated and
restart.

Figure 5 of paper TF-WeM6